

Wavelength-Dependent Photosubstitution and Excited-State Dynamics of $[\text{Cr}(\text{CO})_4(2,2'\text{-bipyridine})]$: A Quantum Yield and Picosecond Absorption Study

Jana Víchová, František Hartl, and Antonín Vlček, Jr.*

Contribution from the J. Heyrovský Institute of Physical Chemistry and Electrochemistry, Czechoslovak Academy of Sciences, Dolejškova 3, 182 23 Prague, Czechoslovakia.

Received May 22, 1992

Abstract: Quantum yields of the photosubstitution of an *axial*-CO ligand in $[\text{Cr}(\text{CO})_4\text{bpy}]$ by PPh_3 were measured as a function of irradiation wavelength, temperature, and solvent. The dependence of quantum yields and of apparent activation energies on the excitation wavelength within the envelope of the metal to ligand charge transfer (MLCT) absorption band points to distinct chemical reactivities for the ligand field (LF) and MLCT excited states. Importantly, it also suggests a photodissociation from higher vibrational levels of directly excited spin-singlet, $^1\text{MLCT}$, electronic excited state(s). This interpretation is corroborated by picosecond transient absorption spectra which show a presence of a short-lived (tens of picoseconds) transient, identified with a $^1\text{MLCT}$ excited state, and a long-lived (≥ 100 ns) transient assigned as a spin-triplet $^3\text{MLCT}$ state. Spectroelectrochemical results indicate a resemblance between the $^1\text{MLCT}$ state and the one-electron reduced species, $[\text{Cr}(\text{CO})_4\text{bpy}]^-$. Comparison of the picosecond spectra measured under 532 (MLCT) and 355 nm (LF) excitation shows that the electronic relaxation of LF states bypasses the $^1\text{MLCT}$ excited state(s), $^1\text{LF}(\text{reactive}) \rightarrow ^3\text{LF}(\text{reactive}) \rightarrow ^3\text{MLCT}(\text{slowly}) \rightarrow ^1\text{ground state}$, whereas the relaxation of $^1\text{MLCT}$ state(s) follows the $^1\text{MLCT}(\text{reactive}) \rightarrow ^3\text{MLCT}(\text{slowly}) \rightarrow ^1\text{ground state}$ pathway.

Introduction

Transition metal complexes and organometallics often possess several excited states of different orbital parentage, which are localized on different parts of the molecule and, at the same time, are in close energetic proximity. Any inefficiency in the communication between such excited states may then give rise to a state-selective photochemical or photophysical behavior which is usually experimentally manifested by a dependence of the photochemical quantum yields^{1,2} or even of the nature of the photoproducts on the excitation wavelength and by a multiple emission.³ For example, substituted pentammine-Ru(II)^{4,5} and pentacyano-Fe(II)⁶ complexes possess metal to ligand charge transfer (MLCT), lowest excited states, and higher-lying ligand field (LF) states. Quantum yields of their photosubstitution reactions sharply decrease going from excitation into the LF absorption band to the MLCT state at lower energies. On the other hand, Ru(II)-diimine complexes exhibit a photosubstitution from the higher-lying ^3LF state that is thermally populated from a long-lived $^3\text{MLCT}$ excited state.⁷⁻⁹ Analogous behavior is also common in the photochemistry of Cr, Mo, and W carbonyls¹⁰⁻¹⁷ containing substituted pyridine ligands. Combinations of excited states other than LF-MLCT are also possible. For example,

specific photochemistry derived from the σ^* , d, σ^* and LF excited states has to be considered in the case of binuclear carbonyl complexes¹⁸ and clusters.¹⁹⁻²¹ Their behavior becomes even more intriguing when two CO ligands in dinuclear complexes are replaced by an α, α' -diimine ligand which introduces MLCT excited states.²²

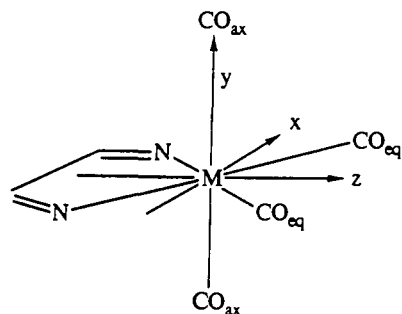
Investigation of the photophysical and photochemical behavior of molecules with several close-lying excited states presents a way to experimentally address some questions which are of fundamental importance for the understanding of the photoreactivity and excited state dynamics in general. In principle, it is possible to obtain information on the relations between the nature of the excited states (orbital configuration, spin) and their reactivity, on the communication between different excited states, and on the partitioning of the electronic excitation energy between different physical as well as chemical (reactive) relaxation channels. Early photochemical events that determine the course of the photochemical processes which are then completed on much longer time scales may thus be investigated. Experimentally, most of the desired information on such competitive state-selective photochemical and photophysical steps may be gained from the excitation-wavelength dependencies of the photochemical quantum yields in combination with very fast time resolved (picosecond to femtosecond) spectroscopic studies using different excitation wavelengths. Measurements of activation parameters, namely activation energies and volumes^{13,23,24} of activation of photochemical reactions at different excitation wavelengths, brings another insight into the problem.

The detailed mechanism of the CO photosubstitutions in substituted transition metal carbonyl complexes in which the lowest-lying excited states have a MLCT character is a long-standing problem in organometallic photochemistry. The cleavage of the W-N bond in $[(\text{CO})_5\text{W-pyrazine-W}(\text{CO})_5]$ was explained¹⁷ by inefficient intrinsic reactivity of the MLCT state. However, the MLCT states were mostly assumed to be unreactive^{16,25} and the

- (1) Langford, C. H. *Acc. Chem. Res.* **1984**, *17*, 96.
- (2) Langford, C. H.; Moralejo, C. In *Photoinduced Electron Transfer*; Fox, M. A., Chanon, M., Eds.; Elsevier: Amsterdam, 1988; Vol. 2, p 420.
- (3) Lees, A. J. *Chem. Rev.* **1987**, *87*, 711.
- (4) Malouf, G.; Ford, P. C. *J. Am. Chem. Soc.* **1974**, *96*, 601.
- (5) Malouf, G.; Ford, P. C. *J. Am. Chem. Soc.* **1977**, *99*, 7213.
- (6) Figard, J. E.; Petersen, J. D. *Inorg. Chem.* **1978**, *17*, 1059.
- (7) Meyer, T. J. *Pure Appl. Chem.* **1986**, *58*, 1193.
- (8) Van Houten, J.; Watts, R. J. *Inorg. Chem.* **1978**, *17*, 3381.
- (9) Durham, B.; Caspar, J. V.; Nagle, J. K.; Meyer, T. J. *J. Am. Chem. Soc.* **1982**, *104*, 4803.
- (10) Wrighton, M. S.; Abrahamson, H. B.; Morse, D. L. *J. Am. Chem. Soc.* **1976**, *98*, 4105.
- (11) Lees, A. J.; Adamson, A. W. *J. Am. Chem. Soc.* **1980**, *102*, 6874.
- (12) Lees, A. J.; Adamson, A. W. *J. Am. Chem. Soc.* **1982**, *104*, 3804.
- (13) Wieland, S.; van Eldik, R.; Crane, D. R.; Ford, P. C. *Inorg. Chem.* **1989**, *28*, 3663.
- (14) Rawlins, K. A.; Lees, A. J.; Adamson, A. W. *Inorg. Chem.* **1990**, *29*, 3866.
- (15) Glyn, P.; Johnson, F. P. A.; George, M. W.; Lees, A. J.; Turner, J. *J. Inorg. Chem.* **1991**, *30*, 3543.
- (16) Geoffroy, G. L.; Wrighton, M. S. *Organometallic Photochemistry*; Academic Press: New York, 1979.
- (17) Lees, A. J.; Fobare, J. M.; Mattimore, E. F. *Inorg. Chem.* **1984**, *23*, 2709.

- (18) Stufkens, D. J. In *Stereochemistry of Organometallic and Inorganic Compounds*; Bernal, J., Ed.; Elsevier: Amsterdam, 1989; Vol. 3, p 226.
- (19) Desrosiers, M. F.; Wink, D. A.; Ford, P. C. *Inorg. Chem.* **1985**, *24*, 1.
- (20) Bentsen, J. G.; Wrighton, M. S. *J. Am. Chem. Soc.* **1987**, *109*, 4518.
- (21) Bentsen, J. G.; Wrighton, M. S. *J. Am. Chem. Soc.* **1987**, *109*, 4530.
- (22) Stufkens, D. J. *Coord. Chem. Rev.* **1990**, *104*, 39.
- (23) van Eldik, R.; Asano, T.; le Noble, W. J. *Chem. Rev.* **1989**, *89*, 549.
- (24) Wieland, S.; Bal Reddy, K.; van Eldik, R. *Organometallics* **1990**, *9*, 1802.

low photoreactivity observed under the visible-light irradiation was often ascribed to the ^3LF states thermally populated from the $^3\text{MLCT}$ ones.^{12,26,27} Although this explanation appears to be valid for many $[\text{W}(\text{CO})_5(\text{pyridine-X})]$ complexes,¹¹⁻¹⁵ the mechanism of the photosubstitution of the *axial*-CO ligand in $[\text{M}(\text{CO})_4(\alpha, \alpha'\text{-diimine})]$, $\text{M} = \text{Cr}, \text{Mo}, \text{W}$, complexes



$[\text{M}(\text{CO})_4(\alpha, \alpha'\text{-diimine})]$

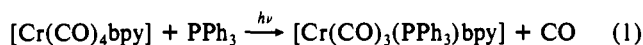
(only part of the diimine ligand is shown)

appears to be rather controversial.^{24-26,28,29} The involvement of ^3LF states has been proposed²⁶ because of the observed temperature dependence of quantum yields. However, recent study²⁴ of the pressure dependence of the photosubstitution quantum yields strongly indicates distinct MLCT and LF reactivities. Indirect evidence for the reactivity of the MLCT state is provided by an electrochemical observation³⁰ that the *axial*-CO ligand is significantly labilized by the ligand-localized reduction to $[\text{M}(\text{CO})_4(\text{bpy}^-)]$ ($\text{bpy} = 2,2'\text{-bipyridine}$). This reduced complex may be regarded as an analogue to the MLCT state formulated approximately as $[\text{M}^1(\text{CO})_4(\text{bpy}^-)]$.

In the present study, the $[\text{Cr}(\text{CO})_4(\alpha, \alpha'\text{-diimine})]$ complexes, namely $[\text{Cr}(\text{CO})_4\text{bpy}]$, were chosen to investigate the reactivity of their LF and MLCT states and to address the more general question of the intrinsic reactivity of MLCT excited states in substituted metal carbonyls. Spectroscopic investigations carried out on various $[\text{M}(\text{CO})_4(\alpha, \alpha'\text{-diimine})]$ complexes^{22,31-34} as well as DV-X α molecular orbital calculation³⁵ on $[\text{Cr}(\text{CO})_4\text{bpy}]$ have actually shown that MLCT states occur as a manifold comprised of several closely spaced excited states making the problem of the MLCT reactivity even more complex.

Results

Quantum yields, ϕ , of the photosubstitution reaction



were measured as a function of the irradiation wavelength λ_{exc} , i.e. excitation energy, $\bar{\nu}_{\text{exc}}$, in four different solvents: $\text{C}_2\text{Cl}_4/\text{C}_6\text{H}_6$ (6/1, v/v, further denoted just as C_2Cl_4), toluene, C_6H_6 , and CH_2Cl_2 . The $[\text{Cr}(\text{CO})_4\text{bpy}]$ complex is strongly solvatochromic,²⁸ and the maximum of its MLCT band lies in these solvents at 565, 535, 529, and 505 nm, respectively. On the other hand, the absorption in the near-UV region ($\bar{\nu} > 23\,000\text{ cm}^{-1}$) which corresponds to predominantly LF transition is nearly solvent inde-

Table I. Quantum Yields ($\times 10^2$)^a of Reaction 1 as a Function of Excitation Wavelength Measured in Different Solvents

λ_{exc} (nm)	CH_2Cl_2	C_6H_6	$\text{C}_6\text{H}_5\text{Me}$	C_2Cl_4^b
362	18.50	19.27	25.41	17.82
419	10.71			
430		12.99		
436	7.95	11.54		8.20
458		9.94		5.80
466		8.70		
479	5.33	7.39		
497		5.70	6.26	4.09
518	3.83	4.22		3.39
528		4.08		3.01
549	2.57	3.00		2.58
557			3.48	1.98
573		2.72		1.93
580	1.70			
599		2.24		1.42
608		1.82		
620		1.65		1.02
639				0.79

^a Average values of at least three measurements. Values calculated according to eq 2. $T = 294.15 \pm 0.1\text{ K}$. ^b $\text{C}_2\text{Cl}_4/\text{C}_6\text{H}_6$, 6/1, v/v mixture.

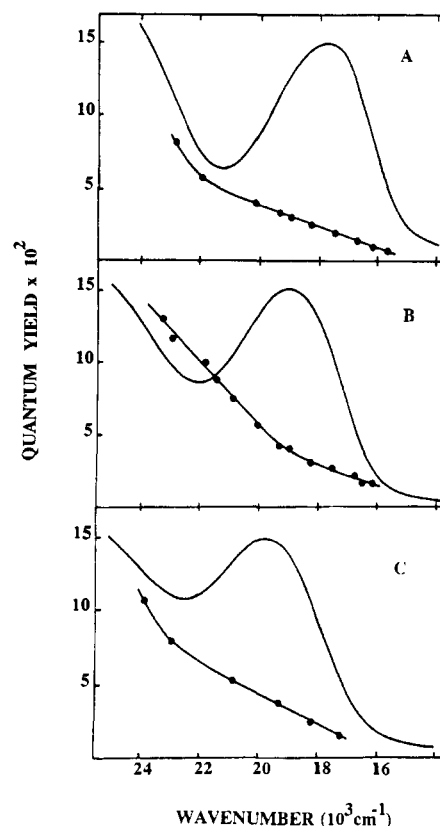


Figure 1. Dependence of quantum yields of reaction 1 on excitation energy and absorption spectra of $[\text{Cr}(\text{CO})_4\text{bpy}]$ measured in different solvents at $21 \pm 0.1\text{ }^\circ\text{C}$: (A) 6:1 (v/v) $\text{C}_2\text{Cl}_4/\text{C}_6\text{H}_6$ mixture, (B) C_6H_6 , (C) CH_2Cl_2 .

pendent. The quantum yield values are summarized in Table I and the wavelength dependencies are depicted, together with the absorption spectra, in Figures 1 and 2. These experiments may be summarized as follows:

(i) Photosubstitution quantum yields decrease sharply with decreasing excitation energy in the near-UV spectral region, where LF absorption dominates, followed by a slow, nearly linear decrease in the visible spectral region of the MLCT absorption. Importantly, the photosubstitution (reaction 1) is quite efficient ($\phi \geq 10^{-2}$) even under excitation into the low-energy onset of the MLCT absorption band.

(ii) The behavior described above is common for all investigated solvents. The ϕ values corresponding to the LF excitation (362

- (25) Wrighton, M. S.; Morse, D. L. *J. Organomet. Chem.* **1975**, *97*, 405.
 (26) Manuta, D. M.; Lees, A. J. *Inorg. Chem.* **1986**, *25*, 1354.
 (27) van Dijk, H. K.; Stufkens, D. J.; Oskam, A. *J. Am. Chem. Soc.* **1989**, *111*, 541.
 (28) Balk, R. W.; Snoeck, T.; Stufkens, D. J.; Oskam, A. *Inorg. Chem.* **1980**, *19*, 3015.
 (29) van Dijk, H. K.; Servaas, P. C.; Stufkens, D. J.; Oskam, A. *Inorg. Chim. Acta* **1985**, *104*, 179.
 (30) Miholová, D.; Vlček, A. A. *J. Organomet. Chem.* **1985**, *279*, 317.
 (31) Staal, L. H.; Stufkens, D. J.; Oskam, A. *Inorg. Chim. Acta* **1978**, *26*, 255.
 (32) Balk, R. W.; Stufkens, D. J.; Oskam, A. *Inorg. Chim. Acta* **1979**, *34*, 267.
 (33) Servaas, P. C.; van Dijk, H. K.; Snoeck, T. L.; Stufkens, D. J.; Oskam, A. *Inorg. Chem.* **1985**, *24*, 4494.
 (34) Rawlins, K. A.; Lees, A. J. *Inorg. Chem.* **1989**, *28*, 2154.
 (35) Kobayashi, H.; Kaizu, Y.; Kimura, H.; Matsuzawa, H.; Adachi, H. *Mol. Phys.* **1988**, *64*, 1009. Note that this paper uses different orientation of x, y, z axes.

Table II. Activation Parameters of Reaction 1 Measured in Toluene

	362 nm	497 nm	557 nm
E_a (cm^{-1})	345 (± 28)	1349 (± 68)	1426 (± 63)
ϕ_0	1.4 (± 1.15)	47.1 (± 1.4)	36.5 (± 1.4)

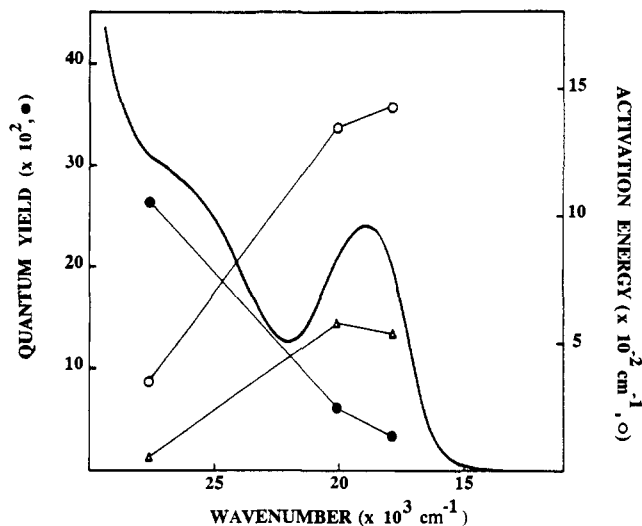


Figure 2. Dependence of quantum yields (at 21 ± 0.1 °C), ϕ (●), activation energies, E_a (○), and preexponential factors, ϕ_0 (Δ), on excitation wavelength in toluene.

nm) depend on the solvent in the following order: toluene \gg C_6H_6 $>$ CH_2Cl_2 $>$ C_2Cl_4 . The absolute differences are, however, very small. At the excitation wavelength corresponding to the maximum of the MLCT absorption, a very similar order was found: toluene $>$ $\text{C}_6\text{H}_6 \approx \text{CH}_2\text{Cl}_2 \gg \text{C}_2\text{Cl}_4$. The same order was found at the red onset of the MLCT absorption. The presence of 10^{-2} M anthracene had no effect on ϕ values.

(iii) The slopes of the linear portion of the ϕ - $\bar{\nu}_{\text{exc}}$ dependencies in the visible spectral region are comparable in C_6H_6 and C_2Cl_4 whereas a somewhat sharper decrease was observed in CH_2Cl_2 and toluene. The behavior in C_6H_6 is exceptional as the region of the sharp fall of ϕ with decreasing $\bar{\nu}_{\text{exc}}$ extends into the high-energy half of the MLCT absorption band ($\bar{\nu} > 19\,500$ cm^{-1}).

The temperature dependence of quantum yields was investigated in toluene at three excitation energies: 27 620, 20 120, and 17 950 cm^{-1} which correspond to 362, 497, and 557 nm, respectively. Quantum yields were measured as a function of the temperature in the range 258–303 K. Experimental values can be fit to linear Arrhenius-type plots according to the following equation: $\phi = \phi_0 \exp(-E_a/RT)$. Actual values are reported in Table II.

The correlation coefficients are very high (0.990 at 362 nm, 0.997 at both 497 and 557 nm). Attempts to fit experimental ϕ values to more complicated equations involving multiexponential terms or a temperature-independent term failed. The dependence of ϕ , ϕ_0 , and E_a on $\bar{\nu}_{\text{exc}}$ is shown in Figure 2.

The presence of two distinct types of photoreactivity is again apparent. Irradiation into the high-energy LF absorption band leads to a photosubstitution characterized by a very low activation energy and low preexponential factor, ϕ_0 . On the other hand, both E_a and ϕ_0 values are much larger for the MLCT-excited photo-reaction. Importantly, the activation energy increases with decreasing $\bar{\nu}_{\text{exc}}$ within the MLCT absorption band and the preexponential factor, ϕ_0 , concomitantly decreases. The observed variations of E_a and ϕ_0 within the MLCT absorption band are significantly larger than experimental errors.

Picosecond absorption spectra were measured in CH_2Cl_2 , pyridine, THF, and toluene. The effects of LF and MLCT excitation were compared using the 355 and 532 nm laser pulses, respectively.

Excitation into the MLCT absorption band at 532 nm produces two transients absorptions: A spectrally-narrow transient absorption, which overlaps with the bleached ground state MLCT

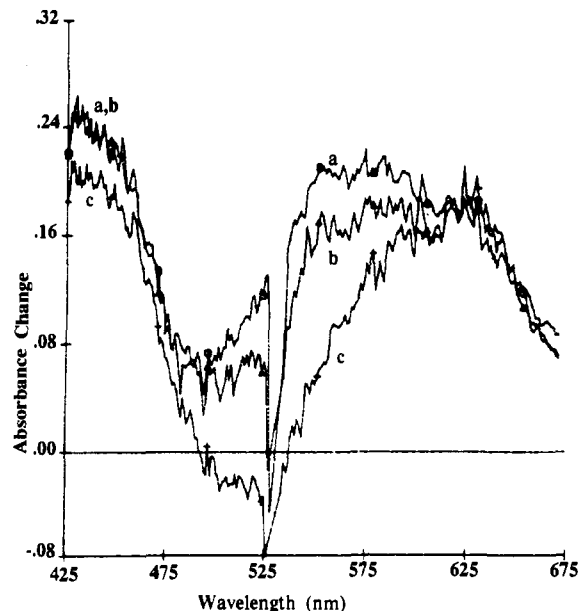


Figure 3. Transient absorption spectra of $[\text{Cr}(\text{CO})_4\text{bpy}]$ measured in pyridine solution at 20 ps (a), 50 ps (b), and 500 ps (c) following laser excitation at 532 nm. The spectrum obtained at 500 ps does not change within the next 10 ns.

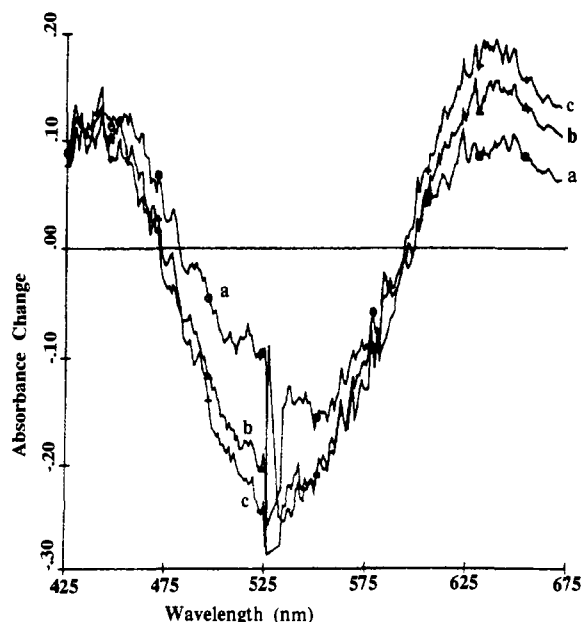


Figure 4. Transient absorption spectra of $[\text{Cr}(\text{CO})_4\text{bpy}]$ measured in toluene solution at 0 ps (a), 50 ps (b), and 10 ns (c) following laser excitation at 532 nm. Spectra measured within the 200 ps to 10 ns time interval were nearly identical.

absorption, is observed at very short times after the excitation. This so called "fast" transient is fully developed within the 30 ps laser pulse excitation. In fact, it was detected at the earliest measurable time delays: -10 ps with respect to the maximum of the time profile of the laser pulse. In pyridine, it is manifested by a decrease in the negative intensity of the bleached ground state MLCT absorption, by a shift of the bleach maximum toward shorter wavelengths, and by a well-developed transient absorption in the 540–575 nm spectral region, see Figure 3.

Analogous shifts of the bleach maximum and decreases of its intensity occur also in toluene and THF. The shift toward longer wavelengths in toluene (Figure 4) and to shorter wavelengths in THF suggests that the maximum of the transient absorption occurs between 450 and 550 nm in toluene and between 480 and 530 nm in THF. Study of the time dependence of the shape and intensity of this "fast" transient absorption spectra in pyridine and

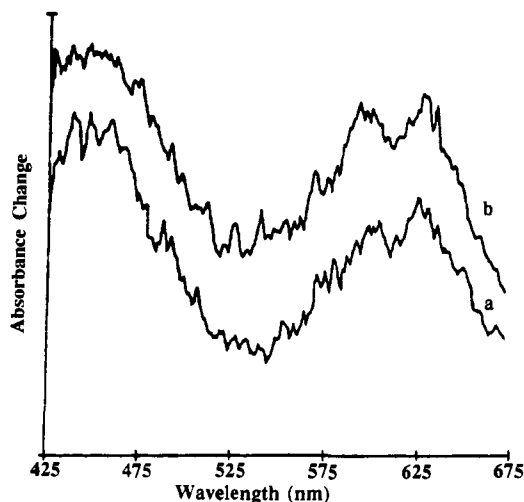


Figure 5. Transient absorption spectra of $[\text{Cr}(\text{CO})_4\text{bpy}]$ measured in toluene solution at 50 ps (a) and 5 ns (b) following laser excitation at 355 nm. (For clarity, curves are shifted with respect to each other. The "dip" at about 620 nm is an experimental artifact.)

toluene shows that its decay is completed within 200 ps. As shown in Figure 3, the intensity of this transient absorption decreases even between 20 and 50 ps. For a sufficiently long-lived transient, an increase is actually expected in this time interval as the sample is still being excited after 20 ps. This observation suggests that only later stages of the decay of the "fast" transient were observed. Its lifetime may thus be estimated as ≈ 50 ps.

The second transient absorption is rather broad, extending over the whole spectral region that was studied (425–675 nm) and overlapping with bleached ground state absorption. It is formed almost completely during the 30 ps excitation pulse and it was detected already at -10 ps. However, its intensity measured in toluene in the red spectral region slightly increases between 50 and 200 ps, concomitantly with the decay of the "fast" transient (see Figure 4). In pyridine, this transient spectrum partly overlaps in the red spectral region with the spectrum of the "fast" transient. However, despite the rapid decrease in the intensity of the absorption due to the latter transient, the total absorbance in the red spectral region stays constant at time delays longer than 20 ps (Figure 3). It appears that the spectrum due to the "fast" transient is for the most part converted into the spectrum of the second transient. No change of the absorption spectra was detected between 200 ps and 10 ns, suggesting a rather long lifetime (≥ 100 ns) for this "slow" transient.

Excitation into the LF absorption band at 355 nm produces only a broad absorption spectrum due to the "slow" transient. The contribution, if any, from the "fast" transient is negligible. The shape and intensity of the absorption spectra obtained 50 ps and 5 ns after 355 nm excitation are nearly identical (Figure 5). A very small shift of the bleach maximum toward shorter wavelengths in pyridine (at 20 ps) and toward longer wavelengths in toluene (at 50 ps) might suggest a very little contribution from the "fast" transient immediately after the 355 nm excitation. However, the magnitude of this effect is comparable with the experimental error. Comparison of the absorption spectra obtained in pyridine at 20 ps using 355 and 532 nm excitation shows that the typical absorption of the "fast" transient at 540–575 nm is definitely missing under the 355 nm excitation as shown in Figure 6. Absorption spectra obtained at 5 ns following both types of excitation are completely identical in all solvents investigated.

For comparison, picosecond absorption spectra of the $[\text{Cr}(\text{CO})_4\text{phen}]$ were also measured. For CH_2Cl_2 solution, 355 nm excitation was used whereas the effect of MLCT excitation at 532 nm was examined in THF and pyridine solutions. For this complex, measurements of transient absorption were complicated by very broad ground state absorption which extended over most of the accessible spectral region. An unresolved broad transient absorption was observed in all cases. The transient signal partly decays within the 50–500 ps time interval without a change in

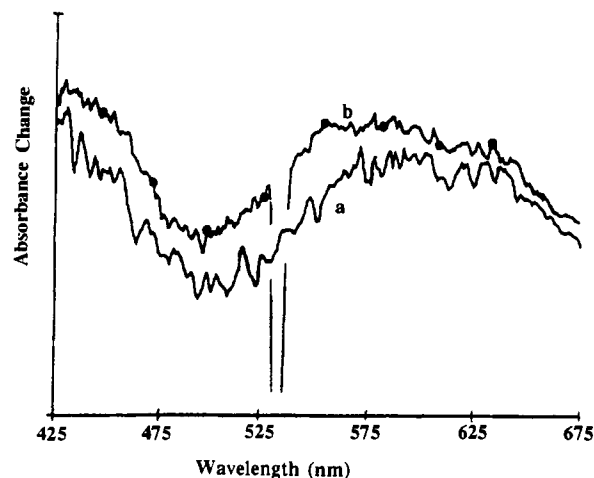


Figure 6. Comparison of transient absorption spectra of $[\text{Cr}(\text{CO})_4\text{bpy}]$ obtained in pyridine solution at 20 ps following 355 nm (a) and 532 nm (b) laser excitation.

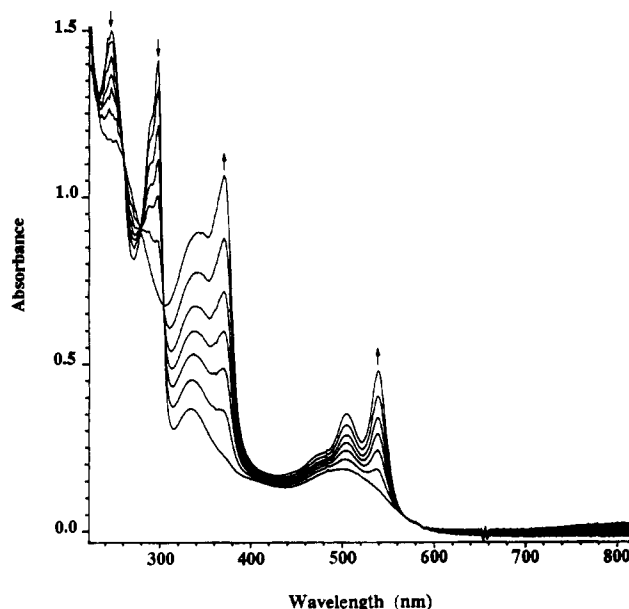


Figure 7. Spectroelectrochemical reduction of $[\text{Cr}(\text{CO})_4\text{bpy}]$ in THF (OTTLE cell, 1.7×10^{-3} M solution containing 10^{-1} M Bu_4NPF_6 , optical length ≈ 0.18 mm).

its shape. The intensity of the transient spectrum then remains nearly constant through the rest of the investigated time interval, i.e. until 5 ns. The fast component of the decay suggests a presence of the "fast" transient analogous to that found for $[\text{Cr}(\text{CO})_4\text{bpy}]$. However, in the case of the phen complex, its spectrum is quite broad, overlapping strongly with that of the "slow" transient.

Spectroelectrochemistry. Both $[\text{Cr}(\text{CO})_4\text{bpy}]$ and $[\text{Cr}(\text{CO})_4\text{phen}]$ are reduced to their corresponding anions in completely reversible one-electron electrochemical processes at -2.13 and -2.12 V, respectively, vs. the ferrocene/ferricinium³⁶ couple. Cyclic voltammetry indicates the chemical stability of the reduced species. The reduction was carried out electrochemically in THF using an optically transparent thin layer electrochemical (OTTLE) cell³⁷ and monitored by UV–vis spectroscopy. The absorption spectrum of $[\text{Cr}(\text{CO})_4\text{bpy}]^-$ (Figure 7) exhibits sharp peaks at 342 nm ($\epsilon = 18\,800 \text{ M}^{-1} \text{ cm}^{-1}$), 370 nm ($\epsilon = 22\,400 \text{ M}^{-1} \text{ cm}^{-1}$), 480 nm (sh), 505 nm ($\epsilon = 7600 \text{ M}^{-1} \text{ cm}^{-1}$) and 538 nm ($\epsilon = 10\,200 \text{ M}^{-1} \text{ cm}^{-1}$) very similar to that³⁸ of free bpy^- which has peaks at

(36) Cagné, R. R.; Koval, C. A.; Lisensky, C. G. *Inorg. Chem.* **1980**, *19*, 2854.

(37) Krejčík, M.; Daněk, M.; Hartl, F. J. *Electroanal. Chem.* **1991**, *317*, 179.

(38) Krejčík, M.; Vlček, A. A. *J. Electroanal. Chem.* **1991**, *313*, 243.

the MLCT states or whether thermal population of reactive LF states is involved. Previously reported pressure dependence of the quantum yields²⁴ of CO photosubstitution in $[\text{M}(\text{CO})_4\text{phen}]$ complexes of W and Mo clearly shows that LF and MLCT states have their own distinct reactivities as the CO substitution occurs dissociatively from LF states and associatively from MLCT states. These experiments are less conclusive for Cr complexes where a dissociative mechanism was found for both LF and MLCT excitation.²⁴ However, much smaller values of the volume of activation, $\Delta V^\ddagger_{\text{MLCT}}$, were found for the CO substitution in $[\text{Cr}(\text{CO})_4\text{phen}]$ using MLCT excitation ($+2.7 \text{ cm}^3 \text{ mol}^{-1}$) than for the LF excitation ($+9.6 \text{ cm}^3 \text{ mol}^{-1}$). This is strong evidence against a reaction from the thermally populated ^3LF state for which $\Delta V^\ddagger_{\text{MLCT}} > \Delta V^\ddagger_{\text{LF}}$ is predicted.^{13,24} The solvent dependence of quantum yields (Figure 1, Table I) also points against thermal population of LF states. The MLCT transition is highly solvatochromic, the MLCT excited states being energetically stabilized in nonpolar solvents. On the other hand, the energy of the LF states (and, hence, also of the LF spectral transition) is solvent independent. The LF-MLCT energy gap may be estimated from the electronic spectra to be by 1110 cm^{-1} larger in toluene than in CH_2Cl_2 . Despite that, the quantum yields measured in toluene in the visible spectral region are higher. Also, if the thermal population of ^3LF states occurred, the observed activation energy should approximately correspond to the energy difference between the $^3\text{MLCT}$ and ^3LF states and the $\ln \phi$ vs $1/T$ dependence should be multiexponential^{8,9} and independent of $\bar{\nu}_{\text{exc}}$ within the MLCT band, contrary to experimental observations. Other evidence is provided by comparison with the photosubstitution of the 4-CN-py ligand in $[\text{W}(\text{CO})_5(4\text{-CN-py})]$ which was conclusively shown^{11,12} to occur from the thermally populated ^3LF state. The value of E_a was found to be 2660 cm^{-1} , and the $^3\text{MLCT}$ lifetime is about $0.3 \mu\text{s}$. If the same mechanism operated for $[\text{Cr}(\text{CO})_4\text{bpy}]$, where $E_a \approx 1400 \text{ cm}^{-1}$, a lifetime of about 600 ps would be predicted for the $^3\text{MLCT}$ excited state, in sharp contrast with $\tau \geq 100 \text{ ns}$ estimated experimentally. Another important observation is an absence of any quenching of reaction 1 by anthracene ($E_T = 1.4 \times 10^4 \text{ cm}^{-1}$) despite the long lifetime and higher energy ($\approx 1.6 \times 10^4 \text{ cm}^{-1}$)²⁶ of the $^3\text{MLCT}$ states. This is good evidence against any involvement of $^3\text{MLCT}$ states in CO photosubstitution.

Most importantly, the ϕ values exhibit a definite dependence on the excitation energy within the MLCT band envelope (Figures 1 and 2), indicating that the reactive excited state still keeps the memory of the primarily populated vibronic state. However, the $^3\text{MLCT}$ states comprise a thermalized manifold of long-lived vibrationally relaxed excited states as was demonstrated³⁴ by emission studies on analogous complexes of Mo and W and, for Cr, by the picosecond experiments described above ("slow" transient). Any information on the original excitation has to be lost in the $^3\text{MLCT}$ manifold unless the efficiency of the population of the $^3\text{MLCT}$ states by ISC from directly excited $^1\text{MLCT}$ states is excitation-energy dependent. The picosecond spectra point away from such a dependence. Due to the solvatochromism of the MLCT transition, the fixed-wavelength 532 nm laser pulse excitation spectra falls into different regions of the MLCT absorption band in different solvents. If the assumption of the excitation energy dependent ISC was correct, a smaller amount of the "slow" transient should be formed in CH_2Cl_2 , pyridine, and THF where the excitation falls into the low-energy side of the absorption band than in toluene where the high-energy side is excited. Although the picosecond measurements in different solvents were repeated several times, no evidence for a systematic difference in transient signal intensity was observed. Also, an excitation-wavelength dependence of the activation energy within the MLCT absorption band is not expected for a reaction from relaxed $^3\text{MLCT}$ states unless the $^1\text{MLCT} \rightarrow ^3\text{MLCT}$ ISC is both a $\bar{\nu}_{\text{exc}}$ -dependent and, at the same time, T -dependent process. However, this is highly improbable as the molecular distortion between these two states is expected to be small and the kinetics of such an ISC can be treated within the weak-coupling limit⁴³ which does not predict

a temperature dependence. It can thus be concluded that all available experimental evidence indicates that the CO photodissociation in $[\text{Cr}(\text{CO})_4\text{bpy}]$ does not occur from the $^3\text{MLCT}$ excited states and that the potentially reactive ^3LF states are not populated when the complex is excited into the MLCT absorption band.

It is proposed that the CO dissociation takes place from directly populated vibrationally excited ("hot") spin-singlet $^1\text{MLCT}$ states (Scheme I). The picosecond spectra has shown that the lifetime of the $^1\text{MLCT}$ states is only a few tens of picoseconds, i.e. shorter than the time required for vibrational relaxation which may take as long as several hundreds of picoseconds.⁴⁴⁻⁴⁶ The assumption of the CO dissociation competing with vibrational relaxation is thus quite realistic. The probability of the CO dissociation is expected to be higher for higher vibrational levels of the reactive $^1\text{MLCT}$ state. The observed dependence of E_a on $\bar{\nu}_{\text{exc}}$ within the MLCT absorption band (Figure 2) is in line with this explanation. For a process originating from vibrationally "hot" states, the overall activation energy depends on the energy of the particular vibrational levels involved.⁴⁷ The values of E_a should thus increase with decreasing vibrational excitation, i.e. with decreasing excitation energy. This was, indeed, observed. However, it also has to be taken into account that $[\text{Cr}(\text{CO})_4\text{bpy}]$ possesses several $^1\text{MLCT}$ states lying in close energetic proximity.^{22,31-35} As the visible absorption band is comprised^{22,31-34} of two or three strongly overlapping bands corresponding to different MLCT transitions, excitation at different $\bar{\nu}_{\text{exc}}$ values may lead to a different initial population of individual $^1\text{MLCT}$ states. They originate in excitation of an electron from either of the three nondegenerate chromium d_x orbitals into either of the three different π^* orbitals of the bpy ligand³⁵ and differ considerably from each other in the extent of the mixing between the d_x and $\pi^*(\text{bpy})$ orbitals, i.e. in the amount of the electron density actually transferred to the bpy ligand. Hence, their reactivity is expected to be different. The observed single-exponential character of the $\ln \phi$ vs $1/T$ plots indicates that the CO dissociation occurs predominantly from a single member of the $^1\text{MLCT}$ manifold. The monotonic decrease of ϕ with $\bar{\nu}_{\text{exc}}$ clearly shows that a higher-lying $^1\text{MLCT}$ state, apparently $13b_2, 14b_2$, is most reactive. The $13b_2 \rightarrow 14b_2$ transition is the most intense^{22,31-35} among all available MLCT transitions. It can thus be excited, with $\bar{\nu}_{\text{exc}}$ -dependent efficiency, throughout the whole region of the MLCT absorption band, as was shown for analogous complexes.³²

It is not quite obvious why the $\text{M}-\text{CO}_{\text{ax}}$ bond is activated in the $^1\text{MLCT}$ state(s). Obviously, depopulation of chromium d_x orbitals diminishes the $\text{Cr} \rightarrow \text{CO}$ π -back-bonding in the MLCT excited state. However, this effect cannot account completely for the labilization of the $\text{Cr}-\text{CO}_{\text{ax}}$ bonds as the back-donation to equatorial CO ligands is diminished as well without labilizing them. In addition, the MLCT photosubstitution quantum yield found²⁶ for $[\text{Cr}(\text{CO})_4(5\text{-NO}_2\text{-phen})]$ is more than 40 times lower than that for $[\text{Cr}(\text{CO})_4\text{bpy}]$ or $[\text{Cr}(\text{CO})_4\text{phen}]$. Although the population of chromium-localized orbitals is the same in MLCT states of all these complexes, the excited electron in $[\text{Cr}(\text{CO})_4(5\text{-NO}_2\text{-phen})]$ is localized mainly on the NO_2 group, far from the reactive $\text{Cr}-\text{CO}_{\text{ax}}$ bonds. Apparently, the excitation of an electron into the $14b_2 \pi^*$ orbital of the bpy ligand has an important labilizing effect on the $\text{Cr}-\text{CO}_{\text{ax}}$ bond. This is manifested also by rather fast thermal CO substitution from the reduced $[\text{Cr}$ -

(44) Elsaesser, T.; Kaiser, W. *Annu. Rev. Phys. Chem.* **1991**, *42*, 83.(45) Yu, S.-C.; Xu, X.; Lingle, R., Jr.; Hopkins, J. B. *J. Am. Chem. Soc.* **1990**, *112*, 3668.(46) Lingle, R., Jr.; Xu, X.; Zhu, H.; Yu, S.-C.; Hopkins, J. B. *J. Phys. Chem.* **1991**, *95*, 9320.(47) Theoretical treatment of the electron transfer from vibrationally non-relaxed excited states has been published.⁴⁸ The model proposed above for the CO dissociation does not imply that the reaction takes place only from the directly excited Franck-Condon state. It should be viewed as a process originating from a manifold of individually reacting vibrational levels whose populations change with time⁴⁸ due to the vibrational relaxation which occurs in parallel with the CO dissociation. The population of individual levels depends, especially in the early times, on the excitation energy.(48) Jortner, J. *J. Am. Chem. Soc.* **1980**, *102*, 6676.(43) Englman, R.; Jortner, J. *Mol. Phys.* **1970**, *18*, 145.

$(\text{CO})_4\text{bpy}]^-$ complex³⁰ which possesses an unpaired electron in the same $14b_2$ orbital as the excited state. The absorption spectrum of the $^1\text{MLCT}$ state resembles that of $[\text{Cr}(\text{CO})_4\text{bpy}]^-$ reflecting similar electron distribution. As was shown above, vibrational excitation is another prerequisite for efficient CO dissociation. In this context, it is important to note the rather small ΔV^{MLCT} value found²⁴ for the CO photosubstitution from the analogous MLCT-excited $[\text{Cr}(\text{CO})_4\text{phen}]$ complex, $+2.7 \text{ cm}^3 \text{ mol}^{-1}$. This observation suggests either some influence of the incoming molecule²⁴ (most probably the solvent) on the labilization of the Cr–CO bond or an “early” transition state²³ whose structure resembles the undissociated excited molecule. The later explanation seems plausible if the reaction occurred from a configuration at or near the Franck–Condon $^1\text{MLCT}$ state as postulated above. Vibrational excitation might provide sufficient distortion of the reacting molecule in the direction of the transition state. This is in accordance with the resonance Raman spectra of various $[\text{M}(\text{CO})_4(\alpha, \alpha'\text{-diimine})]$ complexes,^{22,28,33} including $[\text{Cr}(\text{CO})_4\text{bpy}]$,⁴⁹ measured under MLCT excitation which definitely indicate that the Cr–CO_{ax} bonding is selectively affected by the MLCT excitation, the effect of the $13b_2 \rightarrow 14b_2$ transition being most prominent. It is thus suggested that the interaction between the singly occupied $14b_2 \pi^*$ bpy orbital with the CO orbitals involved in the Cr–CO_{ax} bonding in the vibrationally excited $^1\text{MLCT}$ state is the main factor responsible for the labilization of the Cr–CO_{ax} bond.

On the other hand, the unreactive lowest-lying $^3\text{MLCT}$ states are thermalized, lacking vibrational excitation that appears to be essential for the activation of CO_{ax} ligands. Moreover, the spin-triplet counterpart to the presumably reactive $13b_2, 14b_2$ state is³⁵ the highest-lying member of the $^3\text{MLCT}$ manifold and cannot thus be significantly populated. The MO calculation which includes the configuration interaction³⁵ also shows that the CT character of some of the $^3\text{MLCT}$ states is much lower than that of their $^1\text{MLCT}$ counterparts because of a significant admixture of the bpy-localized $\pi\pi^*$ configurations into the $^3\text{MLCT}$ states. All these factors might account for the observed unreactivity of the $^3\text{MLCT}$ states.

The MLCT photosubstitution quantum yields in $[\text{M}(\text{CO})_4(\alpha, \alpha'\text{-diimine})]$ complexes are known to depend on the metal in the order $\text{Cr} \gg \text{Mo} > \text{W}$.^{24,26,28} Going from Cr to Mo and W, the mechanism changes from dissociative to associative.^{24,29} The change of the mechanism may be explained by faster vibrational relaxation in complexes of heavier metals and, mainly, by increased spin–orbit coupling which facilitates the ISC to the $^3\text{MLCT}$ states. The CO dissociation from the singlets is no longer kinetically competitive. At the same time, the larger size of the metal allows for an associative CO substitution from long-lived $^3\text{MLCT}$ excited states.

A monotonic decrease of the CO photosubstitution quantum yields within a MLCT absorption band envelope has previously been observed for pentacoordinated Fe(0) carbonyl complexes containing the 1,4-diaza-1,3-butadiene²⁷ or 1,4-dimethyltetraazadiene ligand.^{50,51} $[\text{Fe}(\text{CO})_3(\text{R-DAB})]$, $[\text{Fe}(\text{CO})_3(\text{N}_4\text{Me}_4)]$, and $[\text{Fe}(\text{CO})_2(\text{PPh}_3)(\text{N}_4\text{Me}_4)]$. A small increase in E_a within the MLCT absorption band was found for $[\text{Fe}(\text{CO})_3(\text{N}_4\text{Me}_4)]$: 560 cm^{-1} at 436 nm and 770 cm^{-1} at 546 nm. The explanation of the $\phi - \bar{\nu}_{\text{exc}}$ dependence observed for the tetrazadiene complexes was based on a strong coupling between the MLCT excited state and a dissociation continuum.^{50,51} Excitation at higher energies was supposed^{50,51} to populate a more dense manifold of vibronic states, which, within the strong coupling limit, should lead to a more effective reaction, provided that the CO dissociation is competitive with vibrational relaxation. In the present study, we assume a strong coupling between the potential surfaces of the reactive excited state and the dissociated products, apparently MLCT-excited $[\text{Cr}(\text{CO})_3\text{bpy}]$ and CO. However, our interpretation,

which may be valid also for the Fe(0) complexes, is based on a well-defined crossing point between these surfaces which has to be reached by thermal activation from vibronic states. Our results show that the CO dissociation occurs on a time scale of tens of picoseconds which is long enough to acquire thermal activation energy from the medium. Contrary to the approach used for the iron complexes, the model we proposed stresses the importance of the orbital character of the reactive electronic excited state which determines the particular bonds to be broken and the particular vibrations to be activated.

Conclusions

1. The principal relaxation pathways of LF and MLCT excited states are depicted in Scheme I. Deactivation of ^1LF state does not involve $^1\text{MLCT}$ states. The ^1LF state undergoes an ISC to $^3\text{MLCT}$ states, presumably via ^3LF states. Directly excited $^1\text{MLCT}$ states decay partially through corresponding $^3\text{MLCT}$ states. Apparently, ISC is efficient only if it involves states of similar orbital origin whereas conversion between excited states of significantly different orbital parentage is preferred if they have identical total spin.

2. The spin-singlet $^1\text{MLCT}$ excited state(s) of $[\text{Cr}(\text{CO})_4\text{bpy}]$ are, contrary to their spin-triplet counterparts, reactive toward the dissociation of the axial-CO ligand. The CO dissociation from (near) Franck–Condon $^1\text{MLCT}$ states is a thermally activated process which occurs on a time scale of tens of picoseconds (or even shorter) and is competitive with vibrational as well as electronic relaxation. The difference in the chemical reactivity of $^1\text{MLCT}$ and $^3\text{MLCT}$ excited states is caused by the different population of individual members of the manifolds of spin-singlet and triplet states and by the loss of vibrational activation upon thermalization of the triplet states. It is proposed that spin-singlet $^1\text{MLCT}$ excited states may be of much greater and more general importance in organometallic photochemistry than was previously appreciated.

Experimental Section

$[\text{Cr}(\text{CO})_4\text{bpy}]$ and $[\text{Cr}(\text{CO})_4\text{phen}]$ were synthesized by refluxing a toluene solution of $\text{Cr}(\text{CO})_6$ (Aldrich) and the diimine ligand in a 1:1 molar ratio for 2–3 h under argon atmosphere. The crude product precipitated after cooling and was purified by crystallization from a CH_2Cl_2 -isooctane mixture after most of the CH_2Cl_2 was distilled off. The $[\text{Cr}(\text{CO})_3(\text{PPh}_3)\text{bpy}]$ complex was synthesized by refluxing $[\text{Cr}(\text{CO})_4\text{bpy}]$ with PPh_3 in xylene under rigorously anaerobic conditions.³⁰ Purity of complexes was checked by IR and UV–vis absorption spectra and by cyclic voltammetry. PPh_3 (Aldrich) was recrystallized from ethanol. Solvents (Aldrich or Fluka, all spectroscopic grade) were freshly distilled under argon atmosphere and degassed by prolonged bubbling with pure argon just before photochemical experiments.

Hewlett Packard 8452A diode array and Carl-Zeiss-Jena M40 spectrophotometers were used to measure electronic absorption spectra. The reduced complexes for spectroelectrochemical measurements were generated in an IR-OTTLE cell.³⁷ Controlled-potential electrolyses within the OTTLE cell were carried out using a Polarographic analyzer PA4 (Laboratorní přístroje, Prague) which was also used for CV experiments. All potentials are reported with respect to the Fc/Fc^+ couple.³⁶

The samples used to measure quantum yields were prepared under an argon atmosphere in a Schlenk tube with a sealed-on quartz 1 cm spectral cell (Hellma). The sample solutions were completely stable in the dark on a time scale comparable to, or longer than, that of the photochemical experiments. The concentration of $[\text{Cr}(\text{CO})_4\text{bpy}]$ was approximately $3 \times 10^{-4} \text{ M}$ except for the solutions in the $\text{C}_6\text{H}_6/\text{C}_2\text{Cl}_4$ mixture where a concentration of $1.5 \times 10^{-4} \text{ M}$ was used due to low solubility. The PPh_3 concentration was always 10^{-1} M . All quantum yields were measured at $294 \pm 0.1 \text{ K}$. To measure the temperature dependencies, the temperature of the sample solution was controlled within $\pm 0.1 \text{ K}$. Irradiated solutions were magnetically stirred. A double-beam instrument⁵² was assembled from parts supplied by Applied Photophysics, Ltd. The light from a 900W Xe lamp (Model 4960) passed through a $f = 3.4$ high radiance monochromator (Model 7300) and then through a glass interference filter, $\text{fwhm} \approx 5 \text{ nm}$, to achieve needed spectral purity. (The glass plate of the filters also blocked the light of the 2-nd harmonic wavelength. A set of interference filters covering the whole visible spectral region was manufactured in the Astronomic Institute of the

(49) Snoeck, T. L.; Stufkens, D. J.; Vlček, A., Jr. Unpublished results.

(50) Johnson, C. E.; Troglor, W. C. *J. Am. Chem. Soc.* **1981**, *103*, 6352.

(51) Troglor, W. C. In *Excited States and Reactive Intermediates*; ACS Symp. Ser.; Lever, A. B. P., Ed.; American Chemical Society: Washington, DC, 1986; p 177.

(52) Amrein, W.; Gloor, J.; Schaffner, K. *Chimia* **1974**, *28*, 185.

Czechoslovak Academy of Sciences.) A quartz beamsplitter was used to reflect about 10% of the monochromatic light which then passed through a cell containing pure solvent and onto a reference photodetector. The remaining 90% of the beam (10^{-8} – 10^{-9} einstein-s $^{-1}$) passed through the sample solution (volume $V = 3$ mL, optical length $l = 1$ cm) and onto the sample photodetector. Model 6220 integrating photodetectors using a Si-diode and a Rhodamine B quantum counter were used. To achieve high precision, the detectors were calibrated at each individual irradiating wavelength using Aberchrome 540P (400 nm $< \lambda_{\text{exc}} < 550$ nm), 540 ($\lambda_{\text{exc}} = 362$ nm) or 999P ($\lambda_{\text{exc}} > 550$ nm) reversible actinometers⁵³ supplied by Aberchromics, Ltd., Wales, U.K. Absorption spectra were monitored after each irradiation interval of known duration (Δt). Quantum yields were evaluated by two different procedures which afforded, within the experimental error, identical results. Both procedures took into account the decrease of the light absorbance by the photoactive compound due to both its depletion and the increasing inner-filter effect exerted by the photoproduct. The first procedure used only the value of the incident light intensity I_0 as measured by the reference photodetector. The quantum yields were calculated according to the equation²⁶

$$\ln \frac{A - A_\infty}{A_0 - A_\infty} = \frac{\phi I_0 \epsilon l}{V} \int_0^{\Delta t} \frac{1 - 10^{-A}}{A} dt \quad (2)$$

where A , A_0 , and A_∞ are the values of the absorbance at λ_{exc} of the sample solution at time t , before the irradiation, and after the completion of the reaction. ϵ is the extinction coefficient of the starting compound at λ_{exc} . Values of A_∞ were calculated as $\epsilon_p A_0 / \epsilon$ where ϵ_p is an extinction coefficient of the $[\text{Cr}(\text{CO})_3(\text{PPh})_3\text{bpy}]$ photoproduct measured at λ_{exc} . The ϵ_p values were determined from the spectra of authentic samples of $[\text{Cr}(\text{CO})_3(\text{PPh})_3\text{bpy}]$. Alternatively, the number of photons absorbed in each irradiating interval, N , was calculated by subtracting the light intensity passed through the sample (measured by the sample photodetector) from I_0 . The quantum yields can then be evaluated according to the equation

$$\phi = \frac{V}{\epsilon N} \left[(A_0 - A) + A_\infty \ln \left(\frac{A_0 - A_\infty}{A - A_\infty} \right) \right] \quad (3)$$

(53) Kuhn, H. J.; Braslavsky, S. E.; Schmidt, R. *Pure Appl. Chem.* 1989, 61, 187.

where A is the absorbance at the irradiating wavelength measured after the absorption of N moles of photons. In the case of excitation into the isosbestic point, eq 4⁵⁴ was used:

$$\ln \frac{c_0}{c_p} = \frac{\phi I_0}{c_0 V} (1 - 10^{-A_0}) \Delta t \quad (4)$$

where c_0 and c_p are the initial concentration of the photoreactive species and the photoproduct concentration after irradiating interval Δt . These values were determined spectroscopically. Quantum yields were always measured for several irradiating intervals at the beginning of the irradiation when reaction 1 occurred completely isosbesticly. All measurements were repeated at least three times.

Picosecond absorption spectra were obtained using a system⁵⁵ based on a mode-locked Nd/YAG laser and OMA for data collection. The samples were excited either at 355 or 532 nm using 30-ps laser pulses of an average energy of 2.5 mJ per pulse. The spectra were monitored with a 425–675 nm probe pulse. Larger volumes (5–10 mL) of sample solutions were placed in a Schlenk tube with an attached 2 mm spectral cell under nitrogen atmosphere and thoroughly mixed between the measurements. Absorbance at the excitation wavelength was kept within the 0.35–0.55 range. When experiments were performed in pyridine, fresh solutions of identical concentration were used for the measurement of the spectra at each time delay.

Acknowledgment. Picosecond spectra were measured using the facilities of the Canadian Picosecond Laser Center at Concordia University, Montreal. Dr. D. K. Sharma is thanked for his technical assistance. Laser experiments, as well as the stay of one of the authors (A.V.) at Concordia, were financially supported by NSERC. A.V. gratefully acknowledges Prof. C. H. Langford for his great hospitality and for many stimulating discussions. Prof. D. J. Stufkens (Universiteit van Amsterdam) is thanked for his valuable comments. We also acknowledge the generous loan of Aberchrome actinometers from Prof. H. G. Heller, University of Wales, Aberystwyth.

(54) Bunce, N. J. *J. Photochem.* 1987, 38, 99.

(55) Langford, C. H.; Moralejo, C.; Sharma, D. K. *Inorg. Chim. Acta* 1987, 126, 111.

Metal Carbonyl Complexes with Xenon and Krypton: IR Spectra, CO Substitution Kinetics, and Bond Energies¹

Bruce H. Weiller

Contribution from the Mechanics and Materials Technology Center, The Aerospace Corporation, P.O. Box 92957, Los Angeles, California 90009. Received July 9, 1992

Abstract: IR spectra for complexes between Xe and Kr and $\text{M}(\text{CO})_5$ ($\text{M} = \text{Cr}, \text{W}$) have been obtained using laser photolysis of $\text{M}(\text{CO})_6$ and rapid-scan FTIR spectroscopy of liquid rare-gas solutions. The Kr complexes have lifetimes of ~ 0.1 s at 150 K in liquid Kr while $\text{W}(\text{CO})_5\text{Xe}$ has a lifetime of ~ 1.5 min at 170.0 K in liquid Xe. $\text{W}(\text{CO})_5\text{Xe}$ reacts with CO to form $\text{W}(\text{CO})_6$ and the CO substitution kinetics were investigated in liquid Xe over a range of temperatures (173.0–198.0 K) and CO concentrations. The kinetics are consistent with a dissociative substitution mechanism in which $\text{W}(\text{CO})_5\text{Xe}$ is in equilibrium with $\text{W}(\text{CO})_5$. From the temperature dependence of the equilibrium constant, the Xe–W bond energy in $\text{W}(\text{CO})_5\text{Xe}$ is obtained, $\Delta H = 8.4 \pm 0.2$ kcal/mol in good agreement with a recent gas-phase value.

Introduction

The coordinatively-unsaturated, pentacarbonyl fragments, $\text{M}(\text{CO})_5$ ($\text{M} = \text{Cr}, \text{Mo},$ and W), are extremely reactive and form complexes with species normally considered inert such as CF_4 , SF_6 , CH_4 , Ar, Kr, and Xe.² Recent work has focussed on the

complexes with alkanes due to their importance in catalysis and in solution reaction mechanisms.³ However, the ability to form complexes with rare-gas atoms is intriguing and further inves-

(2) Perutz, R. N.; Turner, J. J. *J. Am. Chem. Soc.* 1975, 97, 4791.

(3) (a) Brown, C. E.; Ishikawa, Y.; Hackett, P. A.; Rayner, D. M. *J. Am. Chem. Soc.* 1990, 112, 2530–2536. (b) Dobson, G. R.; Hodges, P. M.; Healy, M. A.; Poliakov, M.; Turner, J. J.; Firth, S.; Asali, K. *J. Am. Chem. Soc.* 1987, 109, 4218–4224. (c) Yang, G. K.; Peters, K. S.; Vaida, V. *Chem. Phys. Lett.* 1986, 125, 566–568.

(1) A preliminary account of this work has been presented: Weiller, B. H. 203rd National Meeting of the American Chemical Society, San Francisco, CA, April 6, 1992.